Structure and relaxation of the trapped magnetic flux in Y-Ba-Cu-O superconductors in magnetic fields below the first critical field H_{c1}

E. V. Blinov
A. F. Ioffe Physico-Technical Institute, 194021, St. Petersburg, Russia

R. Laiho and E. Lähderanta
Wihuri Physical Laboratory, University of Turku, 20500 Turku, Finland

Yu. P. Stepanov and K. B. Traito
A. F. Ioffe Physico-Technical Institute, 194021, St. Petersburg, Russia

(Received 16 May 1994)

Relaxation of the remanent (M_R) and isothermoremanent (M_{IR}) magnetic moment, having the same initial value, is investigated in small superconducting Y-Ba-Cu-O particles in magnetic fields below the first critical field H_{c1}. It is found that the relaxation rate depends strongly on the cooling procedure. A noticeable relaxation of M_{IR} is observed after cooling the sample in zero magnetic field and then applying the magnetizing field. Instead, the value of M_R obtained after cooling the sample in a field proved to be very stable. This result indicates that the structure of the magnetic flux trapped in superconducting particles is different in these two cases. We attribute M_R to a single or a few vortices trapped in the center of superconducting particles, while M_{IR} consists of many short interacting vortices trapped near the surface.

I. INTRODUCTION

High-T_c superconductors display some unusual properties in a wide range of magnetic fields. Intense research has been focused on the structure of the flux-line lattice in fields above the first critical field H_{c1}: the flux-line melting,[1] vortex-glass,[2] and Bose-glass[3] states. On the other hand many exciting features of these materials reveal themselves in lower fields: incomplete Meissner effect,[4–6] paramagnetic Meissner effect,[7,8] hysteresis of the magnetic moment in a field under cooling and warming procedures,[9,10] as well as magnetic-flux trapping and relaxation.[11,12]

An interesting topic of research is the low-field behavior of high-T_c superconductors with dimension d sufficiently small so that the condition

$$H_0 \sim \frac{\phi_0}{d^2} , \tag{1}$$

where H_0 is the magnetizing field and Φ_0 is the magnetic-flux quantum is satisfied.

As was shown in Refs. 13–15 for small superconducting particles the flux-trapping probability is small in a magnetic field less than Φ_0/d^2. This situation has been theoretically investigated for particles much smaller than the London penetration length λ.[15] It is necessary to emphasize that also for $d \gg \lambda$, when the fluxoid quantization condition should be realized, the vortex is not trapped in the particle if $H_0 < \Phi_0/d^2$ because the condition for existence of a vortex is $H_0 = \Phi_0/d^2$.

In our recent work[16] on small Y-Ba-Cu-O particles, no relaxation of the trapped remanent magnetic moment M_R was observed after cooling in a magnetic field (FC) comparable with Φ_0/d^2. Instead, the isothermoremanent moment M_{IR}, having the same initial value and obtained by magnetizing the sample after cooling in zero field (ZFC), reveals a noticeable relaxation. In the present paper a more detailed investigation of this effect is reported. The study of time dependence of the magnetic flux trapped after various cooling and magnetization procedures enables us to conclude that different structures of the trapped magnetic flux are responsible for the different relaxation of M_R and M_{IR}.

II. EXPERIMENTAL DETAILS

The samples were made by crushing and milling sintered $YBa_2Cu_3O_{6.9}$ pellets into powders. The basis material was prepared by annealing for 100 h at 940 °C, 24 h at 906 °C, and 10 h at 400 °C. After this treatment the grain size of the material d_g was more than 50 μm. Powders with classified sizes of the particles were separated by sedimentation in acetone, distinguishing different fractions by the rate of precipitation. Mainly material with particle size of 6–10 μm and total mass 150 mg (sample 1) was used in this work. Some experiments were made also on a 50-mg sample with grain size of 1–6 μm (sample 2) and on a 35-mg specimen with size of the particles between 0.5 and 2.5 μm and prepared from the ceramic material which was annealed for 30 h at 930 °C, 20 h at 907 °C, and 4 h at 400 °C (sample 3).

Magnetic measurements were made with a superconducting quantum interference device (SQUID) magnetometer. Before starting the measurements the remanent field in the sample space was compensated with a superconducting solenoid. A copper solenoid was used to apply a low external dc field H_0. To measure the magnetic

moment the sample was passed through two counterwound pickup coils connected to an RF-SQUID. For time-dependent measurements the specimen was placed inside one of the pickup coils and the SQUID output voltage was recorded as a function of time after removing the magnetizing field H_0. The temperature of the sample was controlled with flowing He gas and measured using a carbon-glass thermometer.

For measurements of M_{IR} the specimen was at first warmed to a temperature about 130 K and then cooled in zero external field down to the measuring temperature. To obtain a uniform temperature over the volume of the sample it was kept in the sample space from 5 to 30 min depending on the temperature. Then the magnetizing field H_0 was applied for some seconds. After switching off H_0 the value of M_{IR} was determined.

For measurements of M_R the specimen was introduced into the sample space quickly when the magnetizing field H_0 was on. After stabilization of the temperature H_0 was removed and M_R or its time dependence were measured.

Special attention was paid to the quality of the specimens, selecting for the measurement only samples which showed no intergranular connections and clustering. This was made by investigating the dependence of M_{IR} on the magnetizing field H_0 to confirm that no shoulder pertaining to intergranular vortices exists in the $M_{IR}(H_0)$ curve.[12]

III. EXPERIMENTAL RESULTS

Figure 1 shows the dependence of the trapped magnetic moment M_{tr} on the magnetizing field H_0 for sample 1.

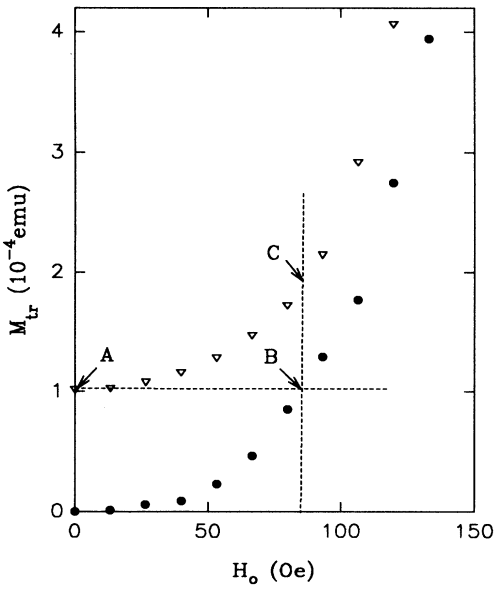

FIG. 1. Dependence of the trapped magnetic moment M_{tr} on the magnetizing field H_0 at 40 K for sample 1. The dots show M_{IR} and the triangles the moment trapped after FC procedure and then adding the field H_0. The meaning of the points *A*, *B*, and *C* is determined in the text.

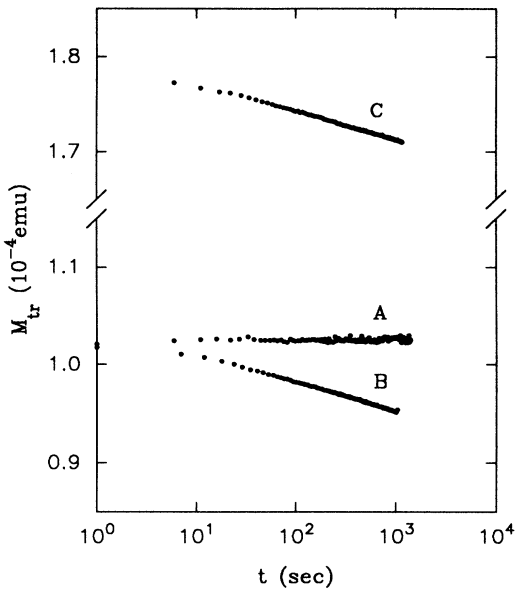

FIG. 2. Time dependence of the trapped magnetic moment M_{tr} after different cooling and magnetizing procedures for sample 1 at 40 K, as discussed in the text.

This experiment has been carried out at 40 K. Data for the isothermoremanent magnetic moment ($M_{tr}=M_{IR}$) are given by dots. The triangles show the moment trapped after first completing the FC procedure and then adding the field H_0. The first data point (*A*) gives the remanent moment after FC in $H_0=1$ Oe. Point *B* corresponds to M_{IR} after applying a field $H_0=85.6$ Oe. The trapped magnetic moment obtained after FC in the field 1 Oe and additional influence of $H_0=85.6$ Oe corresponds to point *C*.

Figure 2 presents the time dependencies of the trapped moment after FC in $H_0=1$ Oe ($M_{tr}=M_R=1.0\times10^{-4}$ emu) shown by point *A* in Fig. 1 (curve *A*) and of the isothermoremanent magnetic moment ($M_{tr}=M_{IR}$) (point *B* in Fig. 1) having the same value 1.0×10^{-4} emu (curve *B*). Curve *C* presents the relaxation of the trapped magnetic moment obtained by adding the magnetization field $H_0=85.6$ Oe after FC in the field of 1 Oe. Qualitatively the same results were obtained for sample 3 at 40 K and sample 1 at 60 K. In all cases after FC in fields comparable with Φ_0/d^2 the trapped moment was quite stable in time. Unlike M_R the isothermoremanent magnetic moment having the same value reveals a noticeable relaxation.

At 40 K no relaxation of M_R was observed using sample 1 up to the field 2.5 Oe. At higher fields the relaxation of the remanent magnetic moment becomes observable. Figure 3 presents the time dependencies of M_R after FC in 5.3 Oe at 30 K (curve 1), 40 K (2), and 60 K (3). In Fig. 4 is shown the relaxation of M_R at the same temperatures 30 K (1), 40 K (2), and 60 K (3) after FC in 10.6 Oe. As can be seen from these figures the relaxation rate of M_R increases with increasing field and temperature.

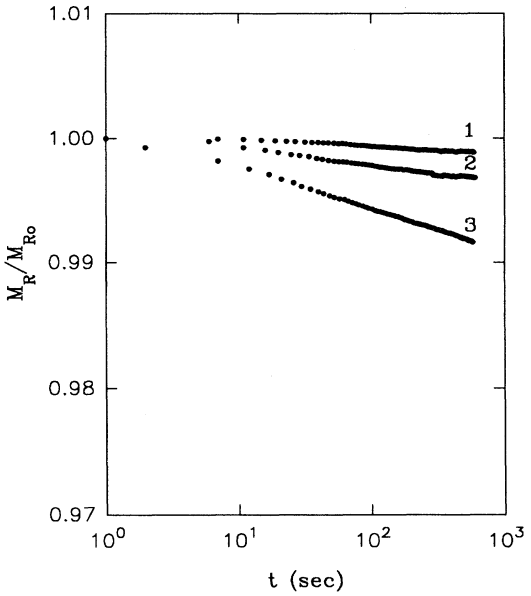

FIG. 3. Time dependencies of M_R after FC in 5.3 Oe at 30 K (1), 40 K (2), and 60 K (3) for sample 1. M_{R0} is the initial value of the trapped moment.

When studying the dependence of M_R on H_0 it was found that M_R does not change with temperature. Figure 5 presents these experimental data at 4 K (triangles) and 40 K (dots) for sample 2. From this picture the value of the threshold field $H_{th}^{FC}=1.8$ Oe can be obtained in a good agreement with the estimated value of $\Phi_0/d^2=0.7-4.5$ Oe for these particles. For fields higher than H_{th}^{FC} a linear relationship between M_R and H_0 is observed.

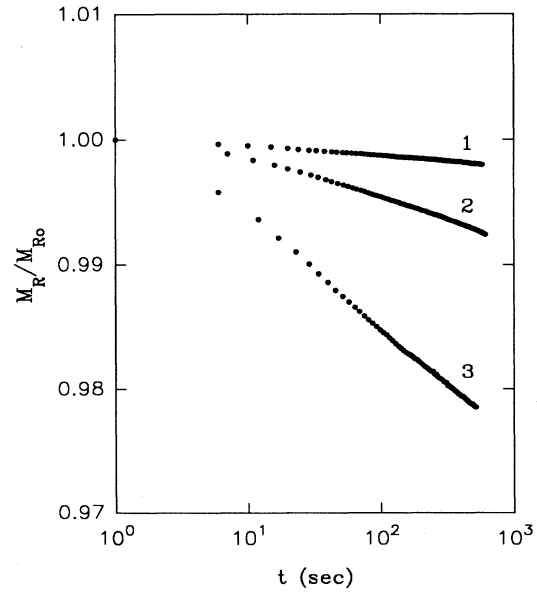

FIG. 4. Relaxation of M_R after FC in 10.6 Oe at 30 K (1), 40 K (2) and 60 K (3) for sample 1. M_{R0} is the initial value of the trapped moment.

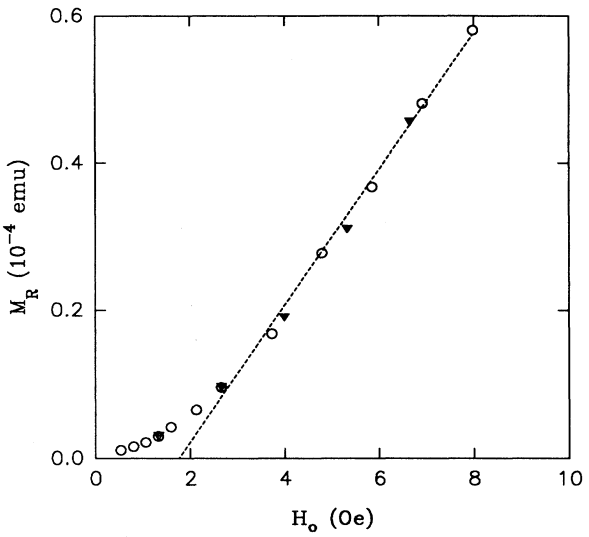

FIG. 5. Dependence of the remanent magnetic moment M_R on the magnetizing field H_0 for sample 2 at 4 K (triangles) and 40 K (circles). The dotted line is to guide the eye.

Unlike M_R, the dependence of the isothermoremanent magnetization on H_0 is sensitive to temperature. The data of M_{IR} obtained for sample 1 at 4 K (open circles), 20 K (filled circles), 40 K (open triangles), and 60 K (filled triangles) are shown in Fig. 6.

IV. DISCUSSION

Magnetic relaxation of type-II superconductors is usually explained by the flux-creep model[17] assuming that the vortices execute thermoactivated jumps with the rate

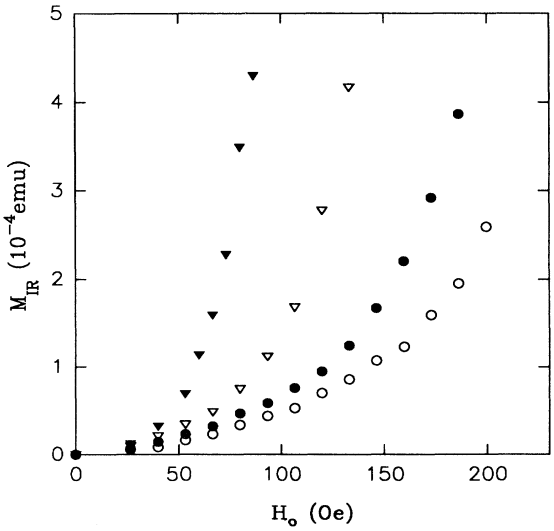

FIG. 6. Dependence of the isothermoremanent magnetic moment M_{IR} on the magnetizing field H_0 for sample at 4 K (open circles), 20 K (dots), 40 K (open triangles), and 60 K (black triangles).

$$V=\omega_0 u \exp\left[-\frac{U(J)}{kT}\right], \quad (2)$$

where ω_0 is a microscopic attempt frequency, u is the distance over which a flux bundle is hopping, k is the Boltzmann constant, T is the temperature, and $U(J)$ is an effective current-dependent activation energy, $U(J)=U_0(1-J/J_c)$, where J_c is the critical current density. The magnetic-flux relaxation can be described by the continuity law of magnetic induction B

$$\frac{\partial B}{\partial t}+\mathrm{rot}[V\times B]=0 . \quad (3)$$

Using Eqs. (2) and (3) one can find the time dependence of the magnetization for different experimental conditions. The case arising most often is the relaxation of the critical-state profile.[18] It has been shown[19] that in this case the magnetization follows the logarithmic time dependence $\delta M(t)\sim\ln(t/\tau)$, where $\tau(\sim 10^{-6}-10^{-3}$ sec) (Refs. 20 and 21) is the characteristic time of the initial relaxation regime. These results have been generalized for a partially critical state,[20–23] for presence of a hump in the critical-state profile,[24] for dependence of the critical current on field,[25–27] and for nonlinear functions of $U(J)$.[21–23,28,29]

From the results in Refs. 20 and 21 one can conclude that the logarithmic time dependence would be observed at $t\geq\tau$ only if the critical-state profile was formed at the initial moment of time. If the initial current J_i is less than the critical current J_c the magnetization will follow the law $m(t)\sim J(t)$ where

$$J(t)=J_c\left[1-\frac{kT}{U_0}\ln\frac{\tau_i+t}{\tau}\right] \quad (4)$$

and $\tau_i=\tau\exp[U(J_i)/kT]$ is the delay time of the relaxation.[21]

The results described above are related to a dense vortex lattice when the interaction between the vortices is not negligible. In the case of a single vortex the magnetization relaxation can be found from a statistical consideration. This problem has been treated in Ref. 30 for ceramics assuming that the vortex escapes from the sample trough the weak-link network. In a homogeneous sample the time dependence of the magnetization follows the diffusion law

$$m(t)=m(0)[1-P(t)] , \quad (5)$$

where $P(t)$ is the probability of the vortex to reach the sample boundary at the time moment t. At the initial relaxation stage $P(t)$ is small and can be estimated from diffusion equation

$$P(t)\sim\exp\left[-\frac{d^2}{4Dt}\right], \quad (6)$$

where D is the diffusion coefficient $[\sim\exp(-U_0/kT)]$. From Eq. (6) it is seen that there is no magnetic moment relaxation for $t\ll t_0=d^2/4D$. Thus the effect of the vortex interaction (nonzero current from adjacent vortices in the vortex core) reveals itself in the value of the delay time. When decreasing J_i the delay time increases from τ in the critical-state limit ($J_i\approx J_c$) to $t_0\approx\tau\exp(U_0/kT)$ in the single-vortex limit ($J_i\approx 0$), resulting in the dependence of the magnetic relaxation rate on the magnetic-flux structure.

Let us consider now our experimental results. One can see that the remanent and the isothermoremanent magnetic moments having the same value (points A and B in Fig. 1) behave in different ways in relaxation experiments (Fig. 2). M_{IR} (curve B in Fig. 2) changes according to the logarithmic law but M_{R} obtained after FC does not change during our experimental time window.

In the case that $M_{\mathrm{tr}}=M_{\mathrm{R}}$ (point A in Fig. 1) the sample is cooled in the field $H_0=1$ Oe. Taking into account that the size of the particles d is some microns, one can conclude that only a single or a few vortices are trapped in every superconducting particle since the magnetic flux penetrating the particle, $\Phi=H_0 d^2$, is approximately equal to the magnetic-flux quantum. These vortices should occupy the places corresponding to the minimum of the Gibbs potential. According to Ref. 13 they are trapped in the particle center. The absence of the relaxation in this case (curve A in Fig. 2) can be explained by Eqs. (5) and (6) which describe the relaxation of single noninteracting vortices.

To estimate the delay time t_0 in this experiment we should know the pinning energy U_0. This energy is characteristic of the pinning center and does not depend on the procedure used for its determination. Therefore one can utilize the data obtained in ZFC procedure (Fig. 2, curve B). Using the formula $d\ln M/d\ln t\approx -kT/U_0$,[19] we find $U_0\sim 100$ kT and $t_0\approx\tau e^{100}$,[100] i.e., there should be no relaxation during the time window of the measurement.

The value of the critical field $H_{c1}^{\perp c}$ is 100–150 Oe at 40 K.[31–34] However, as can be seen from Fig. 1, M_{IR} is observed starting from H_0 of the order 30 Oe. Indeed, in the case of the isothermoremanent magnetization, the magnetic flux can penetrate into the surface irregularities of the particles in a field less than the first critical field H_{c1} and become trapped there as a bundle of surface vortices. In this case the surface critical state is formed. The corresponding theory has been elaborated in Ref. 35. If the height of humps on the surface of the sample is smaller or comparable with their spacing one can assume that the fluxons are approximately straight and point in the same direction as the applied field. Between the humps "lines of force" join the elements of fluxons in the peaks so one can consider the fluxons to be continuous lying partly inside and partly outside the superconductor. If a part $A=A(x)$ of a plane at depth x in the region of surface roughness is occupied by superconductor the mean Gibbs energy per unit volume is

$$G(A)=-\frac{BH_e}{4\pi}+AF(B)+(1-A)\frac{B^2}{8\pi} , \quad (7)$$

where $F(B)$ is the free energy of the vortex lattice[36] and H_e is the external field. Minimizing $G(A)$ with respect to B one can obtain the equilibrium B-H relation for an element of surface at the depth x as

$$H_e = AH_{\rm rev}(B) + (1-A)B \equiv H_r(B, A) \ . \quad (8)$$

Here $H_{\rm rev}(B)$ is the connection between the thermodynamical field and the magnetic induction in the bulk.[36] Using the equation of critical state[37] which connects the Lorentz force F_L and the pinning force $F_p(B, A)$ for a unit length of the fluxon line-of-force system,

$$F_L = -\phi_0 \frac{d}{dx} H(B, A) = \pm F_p(B, A) = \pm \frac{4\pi}{c} J_c(B)\phi_0 A \ , \quad (9)$$

Melville[35] obtained the equation for flux penetration in surface irregularities as

$$\frac{dB}{dx} = \frac{-(dA/dx)(H_{\rm rev} - B) \mp (4\pi/c) A J_c}{1 - A(1 - dH_{\rm rev}/dB)} \ . \quad (10)$$

Signs "−" and "+" in this equation correspond to the increase and decrease of the external magnetic field, respectively.

Equation (10) is analogous to the critical-state equation for the bulk. To obtain an analytical solution of Eq. (10) we use the approximation[38]

$$H_{\rm rev}(B) = fH_{c1} + B \quad (11)$$

with $f = 0.7$ and a simple form of $A(x) = (x/s)^{1/2}$, where s is the characteristic irregularity size (see Appendix). The theoretical expression of $M_{\rm IR}(H_0)$ [see Eq. (A15)] is fitted with experimental data for fields less than H_{c1}. A good result (solid line in Fig. 7) is obtained by using realistic values of the fitting parameters, $H_{c1} = 120$ Oe and $r = 0.1$. As will be shown in the Appendix the trapping of the magnetic flux in the surface irregularities starts after ZFC only if H_0 exceeds a threshold field $H_{\rm th}^{\rm ZFC}$. The value of $H_{\rm th}^{\rm ZFC}$ is found from Fig. 7 to be 25 Oe.

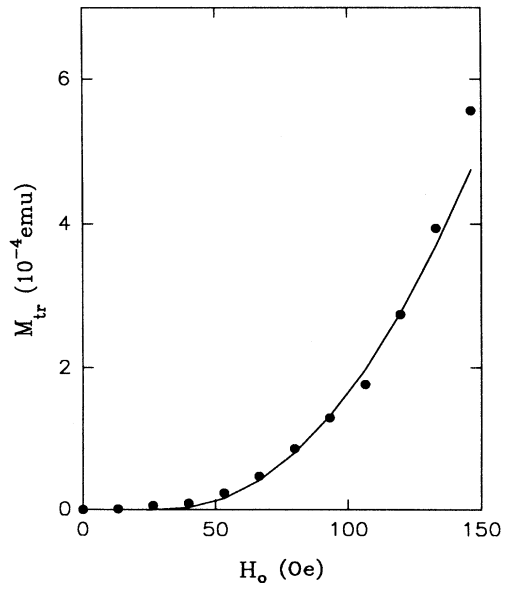

FIG. 7. Experimental data of the isothermoremanent magnetization $M_{\rm IR}$ vs magnetizing field H_0 for sample 1 at 40 K (dots). The solid line gives a plot of $M_{\rm IR}(H_0)$ calculated from Eq. (A15).

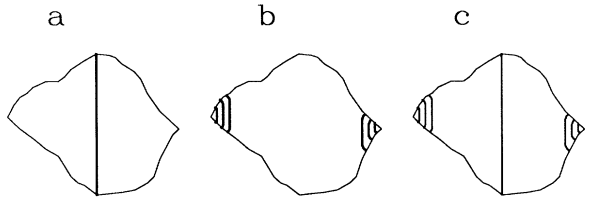

FIG. 8. Structure of the magnetic flux trapped in a small superconducting particle by application of a low magnetic field: $M_{\rm tr} = M_{\rm R}$ (a), $M_{\rm tr} = M_{\rm IR}$ (b), and $M_{\rm tr}$ obtained after combination of FC and an additional magnetization in H_0 (c).

In Figs. 8(a) and 8(b) the structure of the trapped magnetic flux is schematically shown for the remanent and the isothermoremanent magnetic moments, respectively. It can be seen that the surface vortices are considerably shorter than the one situating in the particle center. As a result the same magnetic moment in the cases *a* and *b* correspond to different quantity of vortices. In an FC experiment a single "long" vortex is generated. In the ZFC experiment many "short" surface vortices are trapped in the same particle realizing a "surface" critical state with a surface current approximately equal to the critical current. Then the relaxation is described in Eq. (4) where the delay time τ_i is small because of $U(J_{\rm surf}) \approx 0$ (curve *B* in Fig. 2).

To investigate this idea we consider the relaxation of the trapped magnetic moment obtained by combination of FC in 1 Oe and an additional magnetization in $H_0 = 85.6$ Oe (point *C* in Fig. 1). In this case the trapped moment consists of the "long" vortex in the particle center and of many "short" surface vortices [see Fig. 8(c)]. Because d is larger than the London penetration depth λ ($\lambda_{ab} = 0.14$–0.18 μm in the used temperature range 0–60 K (Ref. 39) and $\lambda_c/\lambda_{ab} = 4.6$ (Ref. 40)), the surface vortices do not interact with the bulk vector. Therefore, although the magnetic moment is approximately two times larger at point *C* than at point *B* the relaxation rates dM/dt (see curves *B* and *C* in Fig. 2) are the same in these two cases. This confirms the assumption about the relaxation of the "surface" critical state and freezing of the single vortex in the particle center.

Our relaxation experiments suggest that the structure of the magnetic moment trapped in low fields is very different in FC and ZFC experiments. However, one can expect that the critical-state profile is formed in FC under increasing the magnetizing field. Then the vortex relaxation should be observed. Let us consider this conjecture in detail.

In the case of the FC process the magnetic flux is uniform over the particle within the framework of the critical-state model and the profile of the trapped flux is similar to that in Fig. 9. Here we consider the situation that the magnetizing field is much less than the Bean penetration field $H^* = (4\pi/c)J_c(d/2)$.[18] Then the screening current J_s ($J_s \approx J_c$) flows near the particle surface and the trapped magnetization is

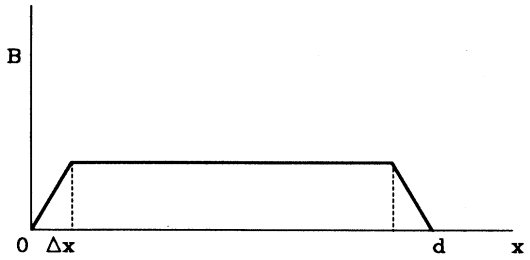

FIG. 9. Density of vortices obtained by the FC process in a superconducting particle with diameter d. The current flows within the layer of thickness Δx on the surface.

$$4\pi m_R = H_0\left[1-\frac{H_0}{(4\pi/c)J_{cd}}\right] = H_0\left[1-\frac{H_0}{2H^*}\right] = H_0\left[1-\frac{\Delta x}{d}\right], \quad (12)$$

where Δx is the thickness of the surface layer in which the current flows. From Eq. (12) one can see that if $H_0 \ll H^*$ then $4\pi m_R \approx H_0$, i.e., the magnetization and magnetic moment do not depend on the current and temperature. This feature is demonstrated in Fig. 5, where the dependencies of M_R on magnetizing field H_0 are shown for $T=4$ K and $T=40$ K. It is also true that the dependence of M_R on H_0 is linear in fields higher than required for the single-vortex creation ($H_0 \approx \Phi/d^2$) in agreement with Eq. (12). The magnetic moment trapped by FC does not depend on J_c and T (Eq. 12). Unlike this case M_{IR} is determined by pinning. Therefore it depends strongly on temperature as shown in Fig. 6.

Equation (12) connects the trapped magnetic moment with the surface current. Then using the expression for the time dependence of the surface current [Eq. (4)] one can obtain the relaxation rate

$$S=-\frac{1}{4\pi M_R}\frac{d4\pi M_R}{d\ln t}\approx\frac{kT}{U_0}\frac{\Delta x(t)}{d}\approx\frac{kT}{U_0}\frac{H_0}{(4\pi/c)J_c d}\,. \quad (13)$$

Because of the small factor $\Delta x(t)/d \ll 1$, Eq. (13) predicts a very slow magnetic relaxation. It results from the fact that only the vortices in the surface layer (where the current is not zero) relax. Therefore with increasing the magnetizing field the thickness of the surface layer enhances resulting in an increase of the relaxation rate. In Figs. 3 and 4 are shown the time dependencies of M_R at different temperatures and magnetic fields. From these pictures one can see that, in agreement with Eq. (13), by increasing the magnetizing field two times, also the relaxation rate is doubled.

The temperature dependence of the relaxation rate which can be obtained from Figs. 3 and 4 is slightly stronger than could be obtained by a linear relationship. This slope can be explained by the decrease of U_0 and J_c when the temperature is increased. One should note that Eq. (13) explains also the observed increase of the relaxation when the size of the particle decreases.[13]

The observed time delays of the relaxation can be caused by two reasons. First, it is due to the difference between J_s and J_c which results in nonzero delay τ_i [see Eq. (4)]. Second, the surface region $\Delta x(t)$ is increased during relaxation resulting in the dependence of the relaxation rate on time and deviation of the relaxation curve from a logarithmic dependence. A similar effect arises in relaxation of a partially critical state as discussed in Refs. 20, 22, and 23.

From comparison of Eqs. (12) and (13) with experimental results one can see that the crossover from a "single-vortex regime" to a "critical-state profile" is realized under increasing of the magnetizing field H_0 in FC. In the former regime the trapped flux is very stable while in the latter regime it shows a slow relaxation, with a rate proportional to H_0.

V. CONCLUSION

We have performed magnetic-flux trapping experiments on superconducting Y-Ba-Cu-O specimens with controlled sizes of particles. Special emphasis is given to the range of fields below the first critical field H_{c1}. It is observed that the flux trapped in low fields to small particles has different structures depending on the cooling and magnetizing procedures. The remanent magnetization observed after FC can be attributed to a single or a few vortices trapped at the center of the superconducting particles and shows practically no relaxation. When the magnetic field is applied after ZFC the penetrating magnetic flux is trapped near the surface. The isothermoremanent magnetization consists in this case of many short interacting vortices and is accompanied by a very noticeable relaxation.

ACKNOWLEDGMENTS

The authors are grateful to Dr. E. B. Sonin for helpful discussions. This work was supported by the Wihuri Foundation and the Russian Science Council on HTC under project No. 93108.

APPENDIX

In this Appendix we derive a formula for $M_{IR}(H_0)$ at $H_0 < H_{c1}$. Substituting Eq. (11) into (10) the reduced surface critical-state equation

$$\frac{dB}{dx}=-\frac{dA}{dx}fH_{c1}\mp A\frac{4\pi}{c}J_c \quad (A1)$$

is obtained. This equation differs from the usual critical-state equation[18] by the additional term $\sim dA/dx$. Due to the negative sign this term acts always in a decreasing external field opposite to the conventional pinning force $\sim J_c$ and results in unusual behavior of the flux distribution.

The variation of the flux distribution when the field is decreased from H_0 to zero is shown schematically in Fig.

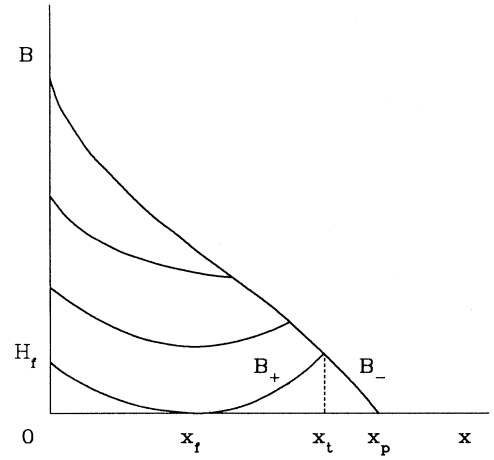

FIG. 10. Variation of the flux distribution in the surface hump $B_+(H_e,x)$ when the external field is decreased from the magnetizing field H_0 to zero. $B_-(H_0,x)$ is the initial flux profile, H_f is the field value at which the vortex-free region starts to form, x_f is the width of the vortex-free region, x_t is the coordinate of the top of the profile, and x_p is the profile penetration depth.

10. This profile differs from the profile determined by the Bean model.[18] Indeed, the existence of the term $\sim dA/dx$ in the right-hand side of Eq. (A1) results in bending of the flux profile near surface humps. If the surface roughness is smooth enough [$A(x)\sim x^\alpha$ with $\alpha<1$], an infinite force occurs at rounded humps on the surface. So the bending increases strongly and a minimum appears in the flux profile. At $H_{ex}=H_f$ when the field in the minimum point of the profile is zero (at $x=x_f$) the flux profile splits into two parts. Under further decreasing of the field the vortices near the surface hump continue to exit, while the vortices from the internal profile are frozen. This results in a vortex-free region up to $x=x_f$ near the surface hump in the zero external field.

Because of the vortex-free region the value of the flux trapped in a low magnetizing field is decreased strongly. If the flux penetration depth $x_p(H_0)\le x_f$ the magnetic flux is not trapped. Therefore there exists a threshold field H_{th}^{ZFC} which can be found from the equation

$$x_p(H_{th}^{ZFC})=x_f \ . \tag{A2}$$

It should be noted that the threshold field H_{th}^{ZFC} is much less than H_{c1}. So one should be careful when determining the value of H_{c1} from the experimental dependence $M_{IR}(H_0)$.

To obtain the function $M_{IR}(H_0)$ we should find $B_-(x)$ and $B_+(x)$ in an increasing and decreasing external field H_e and the characteristic points of the profile: the penetration depth x_p, the vortex-free region x_f, and the coordinate of the profile top x_t (Fig. 10). Note that $B_-(x)$ and $B_+(x)$ refer to the solution of Eq. (A1) with the corresponding signs of the last term. Using $A(x)=(x/s)^{1/2}$ we get from Eq. (A1)

$$B_\mp(H_e,x)=H_e-\left[fH_{c1}\pm\frac{8\pi}{3c}J_c x\right]\left[\frac{x}{s}\right]^{1/2} . \tag{A3}$$

The penetration depth x_p is determined by the condition

$$B_-(H_0,x_p)=0 \ , \tag{A4}$$

and the width of the vortex-free region x_f and the field H_f by the conditions

$$B_+(H_f,x_f)=0 \ , \tag{A5}$$

$$\frac{dB_+}{dx}(H_f,x)|_{x_f}=0 \ . \tag{A6}$$

The top point of the profile is determined from the equality

$$B_+(H_f,x_t)=B_-(H_0,x_t) \ . \tag{A7}$$

From the conditions (A4)–(A7) and Eq. (3) one can find that

$$x_f^*\equiv\frac{x_f}{s}=\frac{r}{2} \ , \tag{A8}$$

$$H_f^*\equiv\frac{H_f}{fH_{c1}}=\frac{2}{3}(x_f^*)^{1/2} \ , \tag{A9}$$

$$x_t^*\equiv\frac{x_t}{s}=[\tfrac{3}{4}(H_0^*-H_f^*)r]^{2/3} \ , \tag{A10}$$

$$x_p^*\equiv\frac{x_p}{s}=(U_++U_-)^2 \ , \tag{A11}$$

$$U_\pm=\{\tfrac{3}{4}rH_0^*\pm[(\tfrac{1}{2}r)^3+(\tfrac{3}{4}rH_0^*)^2]^{1/2}\}^{1/3} \ , \tag{A12}$$

where

$$r=\frac{fH_{c1}}{(4\pi/c)J_c s}, \quad H_0^*=\frac{H_0}{fH_{c1}} \ . \tag{A13}$$

As a result we get

$$4\pi M_{IR}\sim\int_{x_f}^{x_p}B(x)dx=\int_{x_f}^{x_t}B_+(x)dx+\int_{x_t}^{x_p}B_-(x)dx \ . \tag{A14}$$

Substituting Eq. (A3) into Eq. (A14) we have

$$\frac{4\pi M_{IR}}{fH_{c1}s}\sim\frac{3}{5}H_0^*x_p^*-\frac{4}{15}x_p^{*3/2}-\frac{3}{5}(H_0^*-H_f^*)x_t^*-\frac{2}{15}x_f^{*3/2} \ . \tag{A15}$$

Equation (A15) gives $M_{IR}(H_0)$ for magnetizing fields H_0 above the threshold field H_{th}^{ZFC}. In the case $H_0=H_{th}^{ZFC}$ one has $x_p=x_t=x_f$ resulting in $M_{IR}=0$. For $H_0<H_{th}^{ZFC}$ the trapped magnetic moment is zero.

[1]D. R. Nelson, Phys. Rev. Lett. **60**, 1973 (1988).
[2]M. P. A. Fisher, Phys. Rev. Lett. **62**, 1415 (1989).
[3]D. R. Nelson and V. M. Vinokur, Phys. Rev. B **48**, 13 060 (1993).
[4]T. Matsushita, E. S. Otabe, T. Matsuno, M. Murakami, and K. Kitazawa, Physica C **170**, 375 (1990).
[5]S. Ruppel, G. Michels, H. Geus, J. Kallenborn, W. Schlabitz, B. Roden, and D. Wohlleben, Physica C **174**, 233 (1991).
[6]D. Wohlleben, G. Michels, and S. Ruppel, Physica C **174**, 242 (1991).
[7]W. Braunisch, N. Knauf, G. Bauer, A. Kock, A. Becker, B. Freitag, A. Grütz, V. Kataev, S. Neuhausen, B. Roden, D. Khomskii, and D. Wohlleben, Phys. Rev. B **48**, 4030 (1993).
[8]B. Schliepe, M. Stindtmann, I. Nikolic, and K. Baberschke, Phys. Rev. B **47**, 8331 (1993).
[9]J. R. Clem and Z. Hao, Phys. Rev. B **48**, 13 774 (1993).
[10]O. B. Hyun, Phys. Rev. B **48**, 1244 (1993).
[11]A. C. Mota, G. Juri, P. Visani, and A. Pollini, Physica C **162-164**, 1152 (1989).
[12]E. V. Blinov, E. Lähderanta, R. Laiho, and Yu. P. Stepanov, Physica C **199**, 201 (1992).
[13]V. Fleisher, E. Lähderanta, R. Laiho, and Yu. P. Stepanov, Physica C **170**, 161 (1990).
[14]T. J. Jackson, M. N. Keene, W. F. Vinen, and P. Gilberd, Physica B **165&166**, 1437 (1990).
[15]E. V. Blinov, L. S. Vlasenko, Yu. A. Kufaev, E. B. Sonin, Yu. P. Stepanov, A. K. Tagantsev, and V. G. Fleisher, JETP **76**, 308 (1993).
[16]E. V. Blinov, R. Laiho, and E. Lähderanta, Fiz. Tverd. Tela (St. Petersburg) **36**, 1185 (1994) [Phys. Solid State **36**, 649 (1994)].
[17]P. W. Anderson, Phys. Rev. Lett. **9**, 309 (1962).
[18]C. P. Bean, Rev. Mod. Phys. **36**, 31 (1964).
[19]M. R. Beasley, R. Labusch, and W. W. Webb, Phys. Rev. **181**, 682 (1969).
[20]R. Griessen, J. G. Lensink, T. A. M. Schröder, and B. Dam, Cryogenics **30**, 563 (1990).
[21]C. J. van der Beek, G. J. Nieuwenhuys, P. H. Kes, H. G. Schnack, and R. Griessen, Physica C **197**, 320 (1992).
[22]V. M. Vinokur, M. V. Feigel'man, and V. B. Geshkenbein, Phys. Rev. Lett. **67**, 915 (1991).
[23]H. G. Schnack and R. Griessen Phys. Rev. Lett. **68**, 2706 (1992); V. M. Vinokur, M. V. Feigel'man, and V. B. Geshkenbein, *ibid.* **68**, 2707 (1992).
[24]H. G. Schnack, R. Griessen, J. G. Lensink, C. J. van der Beek, and P. H. Kes, Physica C **17**, 337 (1992).
[25]Y. Yeshurun, A. P. Malozemoff, F. H. Holtzberg, and T. R. Dinger, Phys. Rev. B **38**, 11 828 (1988).
[26]M. Xu and D. Shi, Physica C **168**, 303 (1990).
[27]E. V. Blinov, R. Laiho, E. Lähderanta, A. K. Tagantsev, and K. B. Traito, Physica C **222**, 69 (1994).
[28]M. V. Feigel'man, V. B. Geshkenbein, and V. M. Vinokur, Phys. Rev. B **43**, 6263 (1991).
[29]I. M. Babich and G. P. Mikitik, Phys. Rev. B **48**, 1303 (1993).
[30]O. F. Schilling, Phys. Rev. B **44**, 2784 (1991).
[31]L. Krusin-Elbaum, A. P. Malozemoff, Y. Yeshurun, D. C. Cronemeyer, and F. Holtzberg, Phys. Rev. B **39**, 2936 (1989).
[32]V. V. Moshchalkov, J. Y. Henry, C. Marin, J. Rossat-Mignod, and J. F. Jacquot, Physica C **175**, 407 (1991).
[33]D. López, F. de la Cruz, P. Šťastný, N. Leyarovska, and F. C. Matacotta, Phys. Rev. B **47**, 11 160 (1992).
[34]D.-X. Chen, R. B. Goldfarb, R. W. Cross, A. Sanchez, Phys. Rev. B **48**, 6426 (1993).
[35]P. H. Melville, J. Phys. C **4**, 2833 (1971).
[36]P. G. de Gennes, *Superconductivity of Metals and Alloys* (Addison-Wesley, Reading, MA, 1989).
[37]J. Friedel, P. G. de Gennes, and J. Matricon, Appl. Phys. Lett. **2**, 119 (1963).
[38]L. Burlachkov, Y. Yeshurun, M. Konczykowski, and F. Holtzberg, Phys. Rev. B **45**, 8193 (1992).
[39]L. Krusin-Elbaum, R. L. Greene, F. Holtzberg, A. P. Malozemoff, and Y. Yeshurun, Phys. Rev. Lett. **62**, 217 (1989).
[40]M. Yethiraj, H. A. Mook, G. D. Wignall, R. Cubitt, E. M. Forgan, S. L. Lee, D. M. Paul, and T. Armstrong, Phys. Rev. Lett. **71**, 3019 (1993).